http://dx.doi.org/10.5012/bkcs.2012.33.9.3017

Theoretical Approach for the Structures, Energetics and Spectroscopic Properties of $(H_2O_3)_n$ (n = 1-5) Clusters

Hyun-Il Seo, Jin-Ah Bahng, Yeon-Cheol Kim,† and Seung-Joon Kim*

*Department of Chemistry, HanNam University, Daejeon 300-791, Korea. *E-mail: sjkim@hnu.kr*
†Department of Politics, Communication & International Studies, HanNam University, Daejeon 300-791, Korea
Received May 7, 2012, Accepted June 25, 2012

The geometrical parameters, vibrational frequencies, and binding energies for $(H_2O_3)_n$ (n = 1-5) have been investigated using various quantum mechanical techniques. The possible structures of the clusters (n = 2-5) are fully optimized and the binding energies are predicted using energy differences at each optimized geometry. The harmonic vibrational frequencies are also determined and zero-point vibrational energies (ZPVEs) are considered for the better prediction of the binding energy. The best estimation of the binding energy for the dimer is 8.65 kcal/mol. For n = 2 and 3, linear structures with all *trans* forms of the HOOOH monomers are predicted to be the lowest conformations in energy, while the cyclic structures with all *cis*-HOOOH monomers are preferable structures for n = 4 and 5.

Key Words : DFT, HOOOH, $(H_2O_3)_n$, Binding energy

Introduction

Dihydrogen trioxide (HOOOH) is one of the most important intermediates in atmospheric reaction,[1] industrial utility[2] and biochemical oxidations.[3] The interest of HOOOH has been increased recently since it can be more stable ($t_{1/2} \approx 16 \pm 2$ min) than previously believed ($t_{1/2} \approx 20$ ms) in specific solvent such as acetone-d_6.[4]

As a reaction intermediate in the decomposition of hydrogen peroxide (HOOH), HOOOH was first proposed by Berthelot in 1880.[5] After the first investigation of the kinetics of the reaction between ozone and hydrogen peroxide by Rothmund and Burgstaller in 1917,[6] the potential involvement of HOOOH was suggested by several research groups.[7] In 1968 Bielski and Schwartz reported the first UV absorption spectrum of HOOOH in the pulse radiolysis of air-saturated perchloric acid solutions.[8] In 1970 to 1974 the fundamental frequencies of HOOOH were first reported in IR and Raman spectra of the products from electrically dissociated mixture of water, HOOH, and oxygen by Giguère and coworkers.[9] More recent observation of IR spectra of HOOOH has been reported in argon matrices obtained by photolyzing the ozone-hydrogen peroxide mixtures by Engdahl and Nelander in 2002.[10] The preparation of HOOOH in organic solvents was proposed from the ozonation of 1,2-diphenylhydrazine in aceton-d_6 at −78 ºC by Plesnièar *et al*. and confirmed by NMR (^{1}H and ^{17}O) spectra.[11] They also reported that some alkyl hydrotrioxides (ROOOH) of 1,3-dioxolanes decompose to form HOOOH.[12] In 2004 Wentworth and coworkers prepared HOOOH from the thermal reaction of HOOH with ozone in aceton-d_6 at −78 ºC and trioxide was characterized by ^{1}H NMR spectrum.[13] And also in 2005 Suma *et al.* presented the molecular structure of the ground state geometry of HOOOH using Fourier-transform-microwave (FTMW) spectroscopy and FTMW-mm wave method. They confirmed C_2 point group formed a zig-zag skew-chain structure in gas phase.[14]

The first *ab initio* calculation for HOOOH was performed at the low level of theory by Plesnièar *et al*. in 1973.[15] After Plesnièar a number of theoretical investigations on the HOOOH monomer have been reported on the structures and spectroscopic properties.[16-20] In 2002 Xu and Goddard have proposed the reaction mechanism to form HOOOH from the reaction of HOOH with ozone using quantum mechanical method.[2a] In next year Gauss and coworkers reported ^{17}O NMR chemical shift for HOOOH using various theoretical methods.[21] Cremer and coworkers represented the method for the formation of HOOOH as a decomposition product of organometallic hydrotrioxides in acetone-d_6 experimentally and theoretically.[22] In 2008 Plesnièar and coworkers reported the theoretical results for the spectroscopic properties of the dimer, trimer, and tetramer of HOOOH.[23] In next year the theoretical investigation on various hydrogen polyoxides HOOH, HOOOH, HOOOOH, and HOOO have been performed at the very high level of theory, CCSD(T) with the correlation consistent basis sets, by Denis and Ornellas.[24] Tuttle *et al*. reported the theoretical results for the stability and the ^{17}O NMR chemical shift of protonated HOOOH very recently.[25]

In this paper, the geometrical parameters and binding energies for possible $(H_2O_3)_n$ (n = 2-5) clusters have been investigated using various quantum mechanical techniques. Harmonic vibrational frequencies are also predicted using DFT, MP2, and CCSD(T) methods with the aug-cc-pVTZ basis set to confirm that the optimized geometries are true minima or transition states. The binding energies of $(H_2O_3)_n$ (n = 2-5) have been predicted using energy difference at each optimized geometry.

Theoretical Approach

The possible structures of the $(H_2O_3)_n$ (n = 1-5) clusters were fully optimized at the B3LYP[26] level of theory using augmented correlation-consistent polarized valence triple zeta (aug-cc-pVTZ)[27] basis set. Also the new long-range corrected (LC) DFT methods (CAM-B3LYP,[28] LC-ωPBE,[29] ωB97X-D[30]) installed in *Gaussian-09*[31] version had been applied to seek better method to describe the binding energy (ΔE) by comparing with the MP2 result. Harmonic vibrational frequencies were evaluated using analytic second energy derivatives for *cis*- and *trans*-HOOOH at the B3LYP, ωB97X-D, and MP2 levels with the aug-cc-pVTZ basis set and for $(H_2O_3)_n$ (n = 2-5) at the B3LYP/aug-cc-pVTZ level of theory. For *cis*- and *trans*-HOOOH, geometrical parameters and harmonic vibrational frequencies were evaluated using finite displacement method at the CCSD(T)/aug-cc-pVTZ level of theory.

The binding energies were calculated for dimers using all DFT methods mentioned above and MP2 method, while the B3LYP, ωB97X-D, and MP2 methods were applied for the calculation of $(H_2O_3)_n$ (n = 3-5). The MP2 binding energies for n = 3-5 were obtained using single point energy calculation at the B3LYP optimized geometries. The binding energies had been calculated from $E\{(H_2O_3)_n\}-[E(H_2O_3)+E\{(H_2O_3)_{n-1}\}]$. To show H-bonding effect in weakly bounding system, the binding energies had been calculated by the energy differences between monomer and dimer in keeping monomer's geometrical isomer. For example the binding energy of **2c** was calculated from the following equation, $\Delta E(\mathbf{2c}) = E\{(H_2O_3)_2\}-\{E(trans\text{-}H_2O_3)+E(cis\text{-}H_2O_3)\}$. Zero-point vibrational energies (ZPVEs) had been considered to compare with experimental binding energies. The MP2 binding energies for dimer were corrected for the basis set superposition errors (BSSE) using the counterpoise correction method of Boys and Bernardi.[32] The higher-order correlation effect were discussed by comparison of MP2 result with CCSD(T) single point energy. All computations described above were carried out with the *Gaussian09* program packages. The molecular structures were drawn with ORTEP-3 for Windows.[33]

Results and Discussion

Structures.

HOOOH: The structure of HOOOH has been well-characterized experimentally[14] and theoretically[24] and the experimental bond distances of H-O and O-O were determined to be 0.963 Å and 1.428 Å, respectively. In Table 1, the geometrical parameters for HOOOH have been listed at various levels of theory. Two structures (**1a** and **1b**) for HOOOH have been optimized and *trans*-HOOOH (**1a**) is predicted to be lower in energy at all levels of theory employed in this study. The bond lengths of **1a** have been calculated to be 0.970 Å for R(H-O) and 1.427 Å for R(O-O) at B3LYP/aug-cc-pVTZ level of theory and reasonably agree well with the experimental result. The predicted bond angles of 102.0° (∠HOO), 107.9° (∠OOO), and 82.6° (∠HOOO) are also in good agreement with experimental observations of 101.1°, 107.0°, and 81.8°, respectively. At the ωB97X-D/aug-cc-pVTZ level of theory, R(H-O) of 0.965 Å is in better agreement with experimental result but R(O-O) of 1.404 Å is predicted to be 0.024 Å shorter. New DFT method (ωB97X-D) is not helpful to describe the structure of the HOOOH monomer, even though it is useful to characterize the long-range interaction. The predicted bond distances and angles of *cis*-HOOOH are not much different with *trans*-HOOOH except torsional angle (∠HOOO) of 94.6°.

Table 1. Geometrical parameters of $(H_2O_3)_n$ (n = 1, 2) at various levels of theory with the aug-cc-pVTZ basis set

			B3LYP	ωB97XD	MP2
Monomer					
1a	*trans*	R(H-O)	0.970	0.965	0.971
		R(O-O)	1.427	1.404	1.427
		∠HOO	102.1	102.5	100.9
		∠OOO	107.9	107.8	106.8
		∠HOOO	82.6	82.1	82.3
1b	*cis*	R(H-O)	0.970	0.965	0.970
		R(O-O)	1.428	1.405	1.427
		∠HOO	102.4	102.8	101.4
		∠OOO	108.0	107.9	107.0
		∠HOOO	94.6	94.3	94.1
Dimer					
2a	*tt*(chair)	R(H7··O4)	1.879	1.859	1.837
2b	*tt*(boat)	R(H7··O4)	1.902	1.887	1.857
2c	*tc*	R(H10··O1)	1.951	1.934	1.895
		R(H7··O6)	2.032	1.998	1.977
		R(H8··O5)	2.278	2.226	2.137
2d	*cc*(boat)	R(H2··O10)	2.077	2.059	2.028

$(H_2O_3)_n$ (n=2): Total six stable conformations for dimer have been optimized at various levels of theory and four important structures at the B3LYP level are presented in Figure 1. Other structures for dimer are available as supplemental material (Figure S1). Because of the better description of the ωB97X-D method for weakly bound system, the B3LYP hydrogen bond lengths of HOOOH dimer are compared with ωB97X-D and MP2 results in Table 1. In all isomers, the ωB97X-D hydrogen bond lengths are in better agreement with MP2 result than the B3LYP method at the same basis set. The lowest isomer in energy, **2a**, consists of two *trans*-HOOOH monomers combined with two hydrogen bonds to form chair-like eight-membered ring. The hydrogen bond length in **2a** is predicted to be 1.879 Å at the B3LYP level and reduced to be 1.859 Å at the ωB97X-D level, which is close to the MP2 prediction of 1.837 Å. The O-O bond distance involved in hydrogen bonding is elongated by 0.017 Å and the other O-O bond length is decreased by 0.014 Å, as compared with the isolated HOOOH at the B3LYP level. Also the O-H bond distance involved in

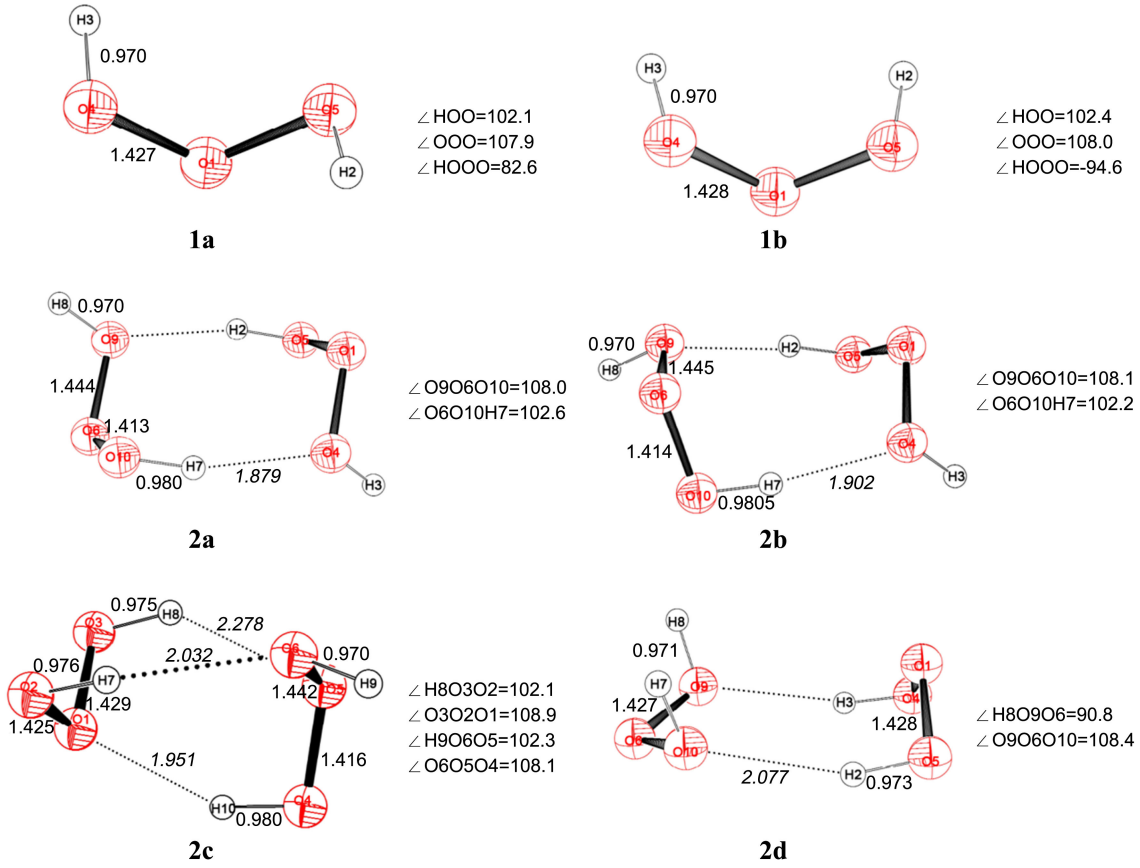

Figure 1. Optimized structures for HOOOH monomers (**1a**, **1b**) and dimers (**2a-2d**) at the B3LYP/aug-cc-pVTZ level of theory. Bond lengths are in Å and bond angles are in degrees.

hydrogen bonding is elongated by 0.010 Å. The next lower isomer in energy, **2b**, consists of two *trans* monomers combined with two hydrogen bonds to form boat-like eight-membered ring. The hydrogen bond distance of 1.857 Å in **2b** is predicted to be significantly longer (by 0.020 Å) than that in **2a** at the MP2 level. The other bond distances and angles in **2b** are similar with those in **2a**. The **2c** structure consists of one *trans* and one *cis* form of HOOOH monomer combined with two normal hydrogen bonds and one additional weak hydrogen bond between middle hydrogen atom (H3) and oxygen atom (O6). The three hydrogen bond lengths in **2c** are predicted to be 1.895, 1.977, and 2.137 Å at the MP2 level. Because of this additional weak interaction, the **2c** isomer is predicted to have the largest binding energy among optimized dimers at all levels of theory except B3LYP level, as shown in Table 2. The **2d** structure consists of two *cis* forms of HOOOH monomer combined with two hydrogen bonds. The hydrogen bond length in **2d** is predicted to be much longer than those in other dimers.

$(H_2O_3)_n$ (n=3): Total eight stable conformations for the HOOOH trimer have been optimized at the B3LYP level and four important structures are presented in Figure 2. Other structures for trimer are available as supplemental material (Figure S2). The lowest conformation (**3a**) in energy has all *trans*-HOOOH monomers in a linear structure combined with two hydrogen bonds to form chair-like eight-membered ring between two consecutive HOOOH monomers. The hydrogen bond lengths in **3a** are predicted to be 1.816 and 1.853 Å at the B3LYP/aug-cc-pVTZ level of theory. The O-H and O-O bond lengths involved in hydrogen bonding are elongated and the other O-O bond distance is shortened as shown in the HOOOH dimer. Next isomer, **3b**, has also all

Table 2. The binding energies of dimers in kcal/mol at various levels of theory with the aug-cc-pVTZ basis set. Values in parentheses are binding energies corrected ZPVE

	B3LYP	CAM-B3LYP	ωB97XD	LC-ωPBE	MP2	MP2(BSSE)[a]
2a	-7.80(-6.18)	-9.39(-7.70)	-9.15(-7.54)	-7.52(-5.99)	-10.43(-8.73)	-9.71(-8.01)
2b	-7.45(-5.78)	-8.93(-7.21)	-8.94(-7.15)	-7.17(-5.58)	-10.16(-8.37)	-9.43(-7.64)
2c	-7.77(-5.86)	-9.69(-7.66)	-9.87(-7.83)	-7.94(-6.11)	-11.35(-9.26)	-10.58(-8.49)
2d	-6.38(-4.86)	-7.80(-6.16)	-8.08(-6.34)	-6.47(-4.99)	-9.05(-7.39)	-8.45(-6.79)

[a]Binding energies corrected 50%-BSSE

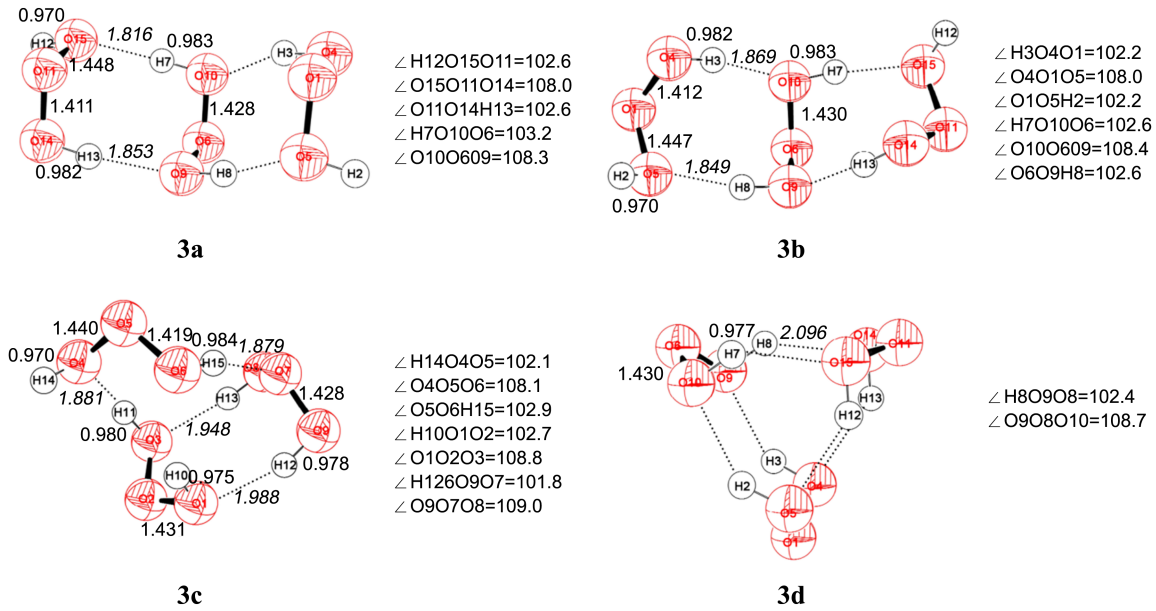

Figure 2. Optimized structures for the HOOOH trimers at the B3LYP/aug-cc-pVTZ level of theory. Bond lengths are in Å and bond angles are in degrees.

trans-HOOOH monomers combined with two hydrogen bonds to form boat-like eight-membered ring between two HOOOH monomers and is very close in energy with **3a**. However, the hydrogen bond lengths in **3b** are predicted to be significantly longer (1.849 and 1.869 Å) than those in **3a**. The third conformation, **3c**, consisted of one *trans*- and two *cis*-HOOOH monomers corresponds to more stable **3b** conformation in the prediction of Plesnièar and coworkers.[23] The hydrogen bond lengths in **3c** are predicted to be in between 1.879 and 1.988 Å. The **3d** trimer has a cyclic

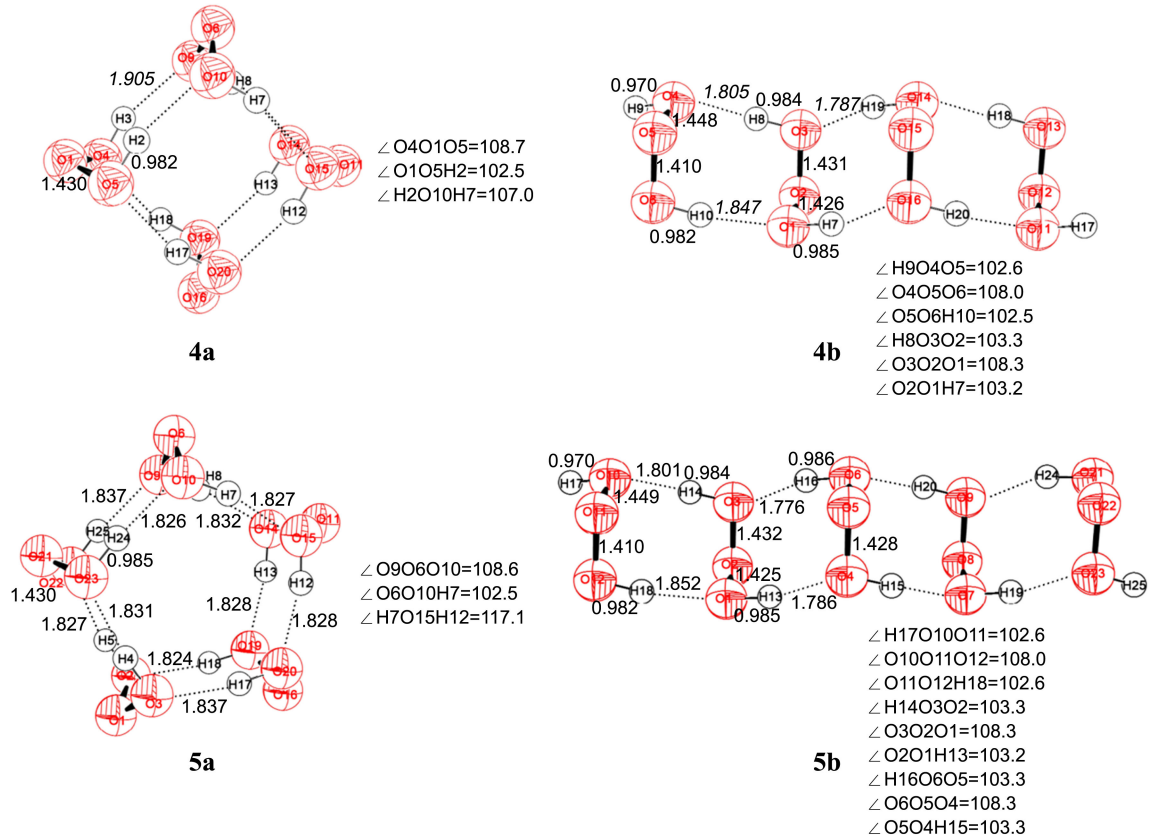

Figure 3. Optimized structures for the $(H_2O_3)_n$ (n=4, 5) at the B3LYP/aug-cc-pVTZ level of theory. Bond lengths are in Å and bond angles are in degrees.

structure with all *cis*-HOOOH monomers combined with six hydrogen bonds. This is our new finding conformation, which has the largest binding energy among nine optimized trimers because of more hydrogen bonds even though they are weakly bound (2.096 Å) in each.

$(H_2O_3)_n$ (n=4-5): For n=4 and 5, four isomers in each are optimized at the B3LYP/aug-cc-pVTZ levels of theory and two important isomers are presented in Figure 3. Other structures for n=4 and 5 are also available as supplemental material (Figure S3). The global minimum of tetramer has the cyclic structure with all *cis*-HOOOH monomers. This conformation also has the largest binding energy optimized in this study because of eight relatively strong hydrogen bonds. That is, the hydrogen bond length (1.905 Å) in **4a** is significantly shorted than that (2.096 Å) in **3d**. The next stable conformation, **4b**, has an open linear structure with all *trans* HOOOH monomers. The hydrogen bond lengths (1.787, 1.805 and 1.847 Å) in **4b** are predicted to be slightly shorter than those in **3a**, which implies stronger hydrogen bonds. The global minimum structure of $(H_2O_3)_5$ retains the cyclic structure with all *cis*-HOOOH monomers. This conformation also has the largest binding energy because of ten strong hydrogen bonds. The hydrogen bond lengths in **5a** are predicted to be much shorter (1.824-1.832 Å) than those in **4a**, which implies increasing binding energy in **5a**. The next stable conformation, **5b**, has an open linear structure with all *trans*-HOOOH monomers. The hydrogen bond lengths (1.776-1.852 Å) in **5b** are predicted to be slightly shorter than those in **4b**.

Binding Energies. We compared the binding energies of HOOOH dimers at various DFT methods (B3LYP, CAM-B3LYP, LC-wPBE, and ωB97X-D) with MP2 result in Table 2. The binding energies of $(H_2O_3)_n$ have been calculated from $E\{(H_2O_3)_n\}-[E(H_2O_3)+E\{(H_2O_3)_{n-1}\}]$. B3LYP binding energies for weakly bound system are usually predicted to be significantly low in comparing with MP2 results. Therefore, the new long-range corrected (LC) DFT methods (CAM-B3LYP, LC-ωPBE, ωB97X-D) have been applied for better description of the binding energy. Among DFT methods, the ωB97X-D binding energies are in the best agreement with MP2 results. For example, the difference in the binding energies predicted by the ωB97X-D and MP2 methods is 1.43 kcal/mol for **2c**, while it is 3.40 kcal/mol between B3LYP and MP2. We are going to use the ωB97X-D method to characterize the binding energies of $(H_2O_3)_n$ (n=3-5) and will compare with the MP2 single-point binding energies calculated at the B3LYP optimized geometries. Table 3 summarizes the binding energies (ΔE) and zero-point vibrational energies (ZPVEs) of $(H_2O_3)_n$ (n=2-5) at various levels of theory and compared. MP2 binding energies are obtained from full optimization for dimers (n=2) and from the single point calculation using the B3LYP optimized geometries for n=3-5.

As shown in Table 3, **2a** structure is the lowest in energy among dimers investigated in this study at all levels of theory. However, the binding energy of **2c** is larger than that of **2a** at the ωB97X-D/aug-cc-pVTZ and MP2/aug-cc-pVTZ levels of theory. This is in consistent with previous theoretical prediction.[23] The ωB97X-D binding energy (9.9 kcal/mol) of **2c** is predicted to be 1.5 kcal/mol lower than MP2 result of 11.4 kcal/mol and is in good agreement with previous theoretical (SCS-MP2) result of 9.22 kcal/mol. After the

Table 3. Absolute energies (E, in hartree), zero-point vibrational energies (ZPVE, in kcal/mol), and relative energies (ΔE, in kcal/mol) for $(H_2O_3)_n$ (n=1-5) clusters at various levels of theory with the aug-cc-pVTZ basis set

			B3LYP			ωB97XD			MP2		
			E	ZPVE	$\Delta E(\Delta E_0)$	E	ZPVE	$\Delta E(\Delta E_0)$	E	ZPVE	$\Delta E(\Delta E_0)$
n=1	**1a**	*trans*	-226.792412	18.9		-226.714473	19.6		-226.390161	19.0	
	1b	*cis*	-226.788694	18.8		-226.710699	19.5		-226.386188	18.9	
n=2	**2a**	*tt*(chair)	-453.597256	39.5	-7.8(-6.1)	-453.443524	40.8	-9.1(-7.5)	-452.796948	39.7	-10.4(-8.7)
	2b	*tt*(boat)	-453.596693	39.5	-7.4(-5.7)	-453.443197	41.0	-8.9(-7.1)	-452.796507	39.8	-10.2(-8.4)
	2c	*tc*	-453.593485	39.7	-7.8(-5.8)	-453.440899	41.1	-9.9(-7.9)	-452.794442	40.0	-11.4(-9.3)
	2d	*cc*(chair)	-453.587555	39.2	-6.4(-4.8)	-453.434274	40.7	-8.1(-6.4)	-452.786790	39.4	-9.0(-7.4)
n=3	**3a**	*ttt*(chair)	-680.404186	60.1	-16.9(-13.5)	-680.175136	62.3	-19.9(-16.4)	-679.204374*		-21.3
	3b	*ttt*(boat)	-680.402675	60.2	-16.0(-12.5)	-680.174044	62.4	-19.2(-15.6)	-679.202996*		-20.4
	3c	*tcc*	-680.397284	60.5	-17.2(-13.2)	-680.170810	62.7	-21.9(-17.9)	-679.199084		-22.9
	3d	*ccc*(ring)	-680.395236	60.3	-18.3(-14.4)	-680.169188	62.4	-23.3(-19.4)	-679.197132*		-24.2
n=4	**4a**	*cccc*(ring)	-907.211735	81.6	-35.7(-29.3)	-906.911731	84.6	-43.3(-36.7)	-905.617182*		-45.5
	4b	*tttt*(chair)	-907.211500	80.7	-26.3(-21.2)	-906.907061	83.5	-30.9(-25.8)	-905.613659*		-33.3
	4c	*tttt*(boat)	-907.208878	80.7	-24.6(-19.5)	-906.905131	83.8	-29.6(-24.2)	-905.611272*		-31.8
	4d	*cccc*(chair)	-907.193530	80.0	-24.3(-19.5)	-906.889282	83.3	-29.2(-23.9)	-905.594429*		-31.2
n=5	**5a**	*ccccc*(ring)	-1134.024980	102.7	-51.1(-42.4)	-1133.649222	106.4	-60.1(-51.2)	-1132.031798*		-63.3
	5b	*ttttt*(chair)	-1134.018807	101.2	-35.6(-28.9)	-1133.639156	105.0	-41.9(-35.0)	-1132.022990*		-45.3
	5c	*ttttt*(boat)	-1134.014977	101.1	-33.2(-26.6)	-1133.636302	105.1	-40.1(-33.1)	-1132.019618*		-43.2
	5d	*ccccc*(chair)	-1133.998828	100.8	-34.7(-27.9)	-1133.619178	104.5	-41.2(-34.2)	-1132.001364*		-44.2

ZPVE corrections, the binding energies of **2c** are reduced to 7.9 and 9.3 kcal/mol at the ωB97X-D/aug-cc-pVTZ and MP2/aug-cc-pVTZ levels of theory. To test the higher-order correlation effect, we performed CCSD(T)/aug-cc-pVTZ single point energy calculation for **2c** and the binding energy of 11.51 kcal/mol increases in magnitude by 0.16 kcal/mol from MP2. The MP2 binding energies were also corrected for the basis set superposition error (BSSE). After 50%-BSSE correction, it is reduced to 10.58 kcal/mol without the ZPVE correction and 8.49 kcal/mol with the ZPVE correction. Therefore the best estimation of the binding energy for the dimer is 8.65 kcal/mol after the ZPVE correction, 50%-BSSE correction, and including higher-order correlation effect.

For n=3, **3a** is predicted to be the global minimum among trimers investigated in this study, however, the binding energies of **3c** and **3d** are larger than that of **3a**. Previously, Plesnièar and coworkers found only two stable isomers for trimers (corresponding to our **3a** and **3c**).[23] The new found **3d** structure has the largest binding energy within trimers investigated in this study because of more hydrogen bonds even though they are weakly bound in each. Predicted binding energy (23.3 kcal/mol) of **3d** at the ωB97X-D level of theory is only 0.9 kcal/mol lower than that (24.2 kcal/mol) of at the MP2 level of theory. The binding energy is predicted to be 19.4 kcal/mol for **3d** at the ωB97X-D level after the ZPVE correction.

For n=4 and 5, the cyclic structures with all *cis*-HOOOH monomers (**4a** and **5a**) are predicted to be the global minima and also have the largest binding energies among isomers optimized in this study. Their binding energies are significantly increased because they have more hydrogen bonds and individual interactions are relatively strong. Predicted binding energies of **4a** and **5a** are 43.3 and 60.1 kcal/mol at the ωB97X-D level of theory. The MP2 binding energies are predicted to be 2.2 kcal/mol for **4a** and 3.2 kcal/mol for **5a** greater than those of ωB97X-D. After the ZPVE correction, the binding energies of **4a** and **5a** are reduced to 36.7 and 51.2 kcal/mol, respectively, at the ωB97X-D level.

The binding energies per unit HOOOH monomer are increasing from n=2 going to n=5, which implies that the longer chain clusters are more favorable. The binding energies per H-bond in linear trans(chair) form are predicted to be 3.75 kcal/mol for dimer (**2a**), 4.10 kcal/mol for trimer (**3a**), 4.30 kcal/mol for n=4 (**4b**), and 4.38 kcal/mol for n=5 (**5b**) at the ωB97X-D/aug-cc-pVTZ level of theory after ZPVE correction. In cyclic *cis*(ring) form, the binding energies per H-bond of 4.6 kcal/mol for n=4 (**4a**) and 5.1 kcal/mol for n=5 (**5a**) are more significantly increased relative to those in dimer (**2c**, 3.20 kcal/mol) and trimer (**3d**, 3.23 kcal/mol) at the same level of theory.

Vibrational Frequencies and Intensities. The calculated harmonic vibrational frequencies of HOOOH at various levels of theory are listed in Table 4 and compared with the experimental result. The experimental IR spectrum of HOOOH has been observed in argon matrices by Engdahl and Nelander.[10] The direct comparison of the present theoretical frequencies with experiment is difficult because the experimental frequencies include anharmonic contributions, while the computed frequencies are harmonic. New long-range corrected (LC) DFT method (ωB97X-D) is not helpful to describe the IR spectrum of HOOOH. The harmonic frequencies are overestimated about 5% for B3LYP and MP2, and 4% for CCSD(T) relative to experimental frequencies except symmetric O-O stretching mode. The B3LYP

Table 4. Harmonic vibrational frequencies of HOOOH (*trans* and *cis*) at various levels of theory with aug-cc-pVTZ basis set in wavenumbers

	B3LYP	ωB97XD	MP2	CCSD(T)	expt.[a]
trans					
symm tors	371.6	369.6	361.5	362.7	346.4
antisymm tors	423.5	427.7	416.5	413.7	387.0
OOO bend	526.3	560.5	535.0	522.5	509.1
antisymm OO stretch	800.4	901.6	827.5	800.2	776.3
symm OO stretch	941.4	1004.9	913.3	895.6	821.0
symm OOH bend	1384.6	1420.8	1385.4	1385.7	1347.4
antisymm OOH bend	1392.7	1430.0	1393.0	1388.9	1359.1
antisymm OH stretch	3703.3	3787.7	3734.6	3726.5	3529.6
symm OH stretch	3707.7	3791.4	3736.8	3730.1	3529.6
cis					
antisymm tors	228.7	293.6	263.5	272.0	
symm tors	446.4	449.2	437.8	437.8	
OOO bend	513.1	547.2	519.4	503.7	
antisymm OO stretch	802.2	904.2	829.0	797.1	
symm OO stretch	941.5	1005.9	915.1	896.9	
antisymm OOH bend	1367.3	1403.6	1368.0	1363.7	
symm OOH bend	1399.6	1437.8	1400.1	1398.5	
symm OH stretch	3701.0	3785.8	3734.3	3723.2	
antisymm OH stretch	3703.5	3788.9	3738.5	3726.6	

[a]Reference 10

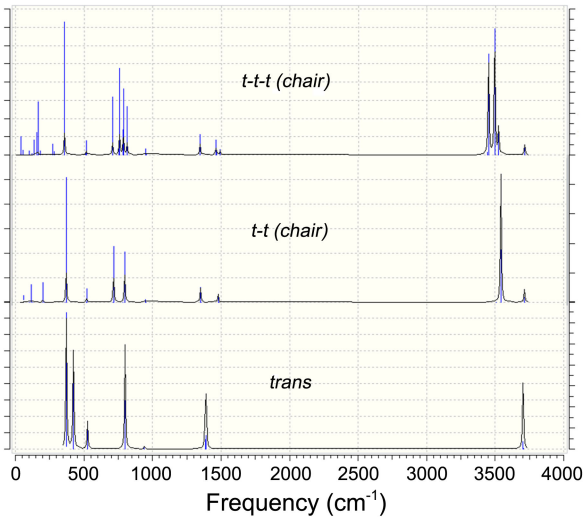

Figure 4. Predicted IR Peaks for the HOOOH monomer (*trans*), dimer (**2a**), and trimer (**3a**) at the B3LYP/aug-cc-pVTZ level of theory.

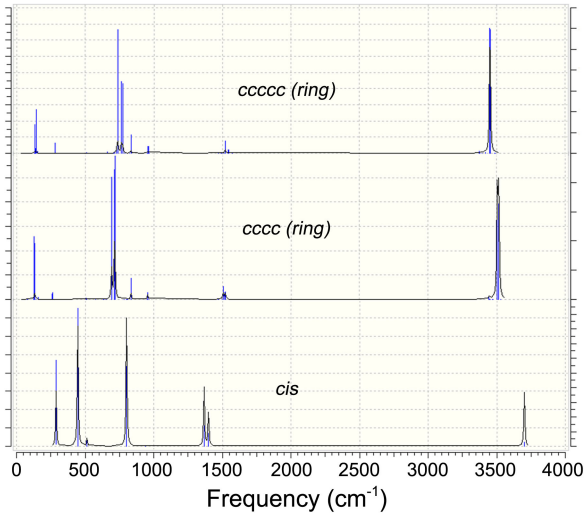

Figure 5. Predicted IR Peaks for the HOOOH monomer (*cis*) and clusters (**4a** and **5a**) at the B3LYP/aug-cc-pVTZ level of theory.

frequencies are reasonably good within harmonic postulation.

In Figure 4, the harmonic vibrational frequencies of *trans*-HOOOH (**1a**) are compared with the results for all trans dimer (**2a**) and trimer (**3a**) at the B3LYP/aug-cc-pVTZ level of theory. As shown in Figure 6, the general feature of the frequencies is red shift of 150-200 cm^{-1} for the O-H stretching mode in dimer and trimer, while the highest frequency transitions are almost unchanged. The OOH bending frequencies (around 1400 cm^{-1}) in monomer are blue shifted by about 100 cm^{-1} (see Figure 6) in dimer and trimer for the OOH bending mode involved in H-bond, while other OOH bending frequencies are not affected too much. The antisymetric O-O stretching modes in monomer are split to multi peaks and red shifted in dimer and trimer for the O-O stretching modes involved in H-bond. There are no significant shifts in the torsional bending modes, while new peaks assigned to ring torsional modes formed from H-bonds arise under 300 cm^{-1}.

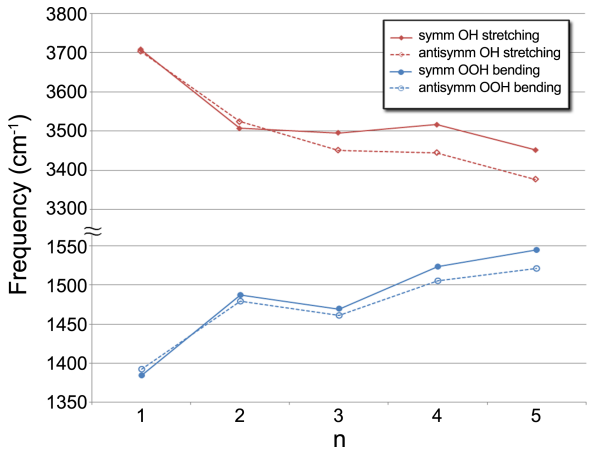

Figure 6. Frequency shifts for the OH stretching and OOH bending modes due to increasing the HOOOH monomer from n=1 to n=5.

In Figure 5, the harmonic vibrational frequencies of the *cis*-HOOOH monomer (**1b**) are compared with the predictions of all *cis* form ring clusters (**4a** and **5a**) at the B3LYP/aug-cc-pVTZ level of theory. As also shown in Figure 6, the similar trends in the red and blue shifts of the O-H stretching and OOH bending modes were observed in **4a** and **5a**. However, more significant red shifts (200-300 cm^{-1}) are observed for the O-H stretching modes because of the strong interactions in **4a** and **5a** relative to those in dimer and trimer. And also because all hydrogens in **4a** and **5a** are involved in H-bonds, all O-H stretching and OOH bending modes are shifted. The torsional bending modes are significantly blue shifted, while there are no significant shifts in the O-O stretching modes. New peaks around 150 cm^{-1} in **4a** and **5a** can be assigned to ring torsional modes formed from H-bonds.

Conclusions

The geometrical parameters, binding energies, and harmonic vibrational frequencies for possible $(H_2O_3)_n$ (n=2-5) clusters have been investigated using various quantum mechanical techniques. For n=2 and 3, linear structures (**2a** and **3a**) with all *trans* forms of the HOOOH monomers are predicted to be the lowest conformations in energy, while **2c** and **3d** isomers have larger binding energies relative to those in **2a** and **3a**. However, for n=4 and 5, the cyclic structures (**4a** and **5a**) with all *cis*-HOOOH monomers are preferable structures and also have the largest binding energies among isomers optimized in this study.

The best estimation of the binding energy for the dimer is 8.75 kcal/mol after the ZPVE correction, 50%-BSSE correction, and including higher-order correlation effect. The binding energies per unit HOOOH monomer are increasing from n=2 going to n=5, which implies that the longer chain clusters are more favorable. The binding energies per H-bond are predicted to be 3.75 kcal/mol for dimer, 4.10 kcal/mol for trimer, 4.30 kcal/mol for n=4, and 4.38 kcal/mol for n=5 in linear *trans*(chair) form at the ωB97X-D/aug-cc-pVTZ level of theory after ZPVE correction. In cyclic *cis*(ring) form, the binding energies per H-bond for **4a** (4.6 kcal/mol) and **5a** (5.1 kcal/mol) are more significantly increased relative to those in dimer (3.20 kcal/mol) and trimer (3.23 kcal/mol) at the same level of theory.

The vibrational frequencies are red shifted for the O-H stretching modes and blue shifted for the OOH bending modes involved in H-bond of dimer (**2a**) and trimer (**3a**), while the highest frequency transitions and other OOH bending frequencies are almost unchanged. The similar trends in the red and blue shifts of the O-H stretching and OOH bending modes were observed in **4a** and **5a**.

Acknowledgments. This research was supported by Basic Science Research Program through the National Research Foundation of Korea (NRF) funded by the Ministry of Education, Science and Technology (Grant No. 2010-0022978).

References

1. Zheng, W.; Jewitt, D.; Kaiser, R. I. *Phys. Chem. Chem. Phys.* **2007**, *9*, 2556.
2. (a) Xu, X.; Goddard, W. A., III. *Proc. Natl. Acad. Sci. U.S.A.* **2002**, *99*, 15308. (b) Maetzke, A.; Jensen, S. J. K. *Chem. Phys. Lett.* **2006**, *425*, 40.
3. (a) Wentworth, P., Jr.; Wentworth, A. D.; Zhu, X. Y.; Wilson, I. A.; Janda, K. D.; Eschenmoser, A.; Lerner, R. A. *Proc. Natl. Acad. Sci. U.S.A.* **2003**, *100*, 1490. (b) Shukla, P. K.; Mishra, P. C. *J. Phys. Chem. B* **2007**, *111*, 4603.
4. Plesnièar, B. *Acta Chim. Slov.* **2005**, *52*, 1.
5. Berthelot, M. *Compt. Rend*. **1880**, *90*, 656.
6. Rothmund, V.; Burgstaller, A. *Monatsh. Chem*. **1917**, *38*, 295.
7. (a) Bray, W. C. *J. Am. Chem. Soc.* **1938**, *60*, 82. (b) Taube, H.; Bray, W. C. *J. Am. Chem. Soc.* **1940**, *62*, 3357.
8. Bielski, B. H. J.; Schwarz, H. A. *J. Phys. Chem*. **1968**, *72*, 3836-3841.
9. (a) Giguèere, P. A.; Herman, K. *Can. J. Chem*. **1970**, *48*, 3473-3482. (b) Deglise, X.; Giguèere, P. A. *Can. J. Chem*. **1971**, *49*, 2242-2247. (c) Arnau, J. L.; Giguèere, P. A. *J. Chem. Phys*. **1974**, *60*, 270-273.
10. Engdahl, A.; Nelander, B. *Science* **2002**, *295*, 482.
11. Plesnièar, B.; Tuttle, T.; Cerkovnik, J.; Cremer, D. *J. Am. Chem. Soc.* **2003**, *125*, 11553.
12. Tuttle, T.; Cerkovnik, J.; Plesnièar, B.; Cremer, D. *J. Am. Chem. Soc.* **2004**, *126*, 16093.
13. Nyffeler, P. T.; Boyle, N. A.; Eltepu, L.; Wong, C.-H.; Eschenmoser, A.; Lerner, R. A.; Wentworth, P., Jr. *Angew. Chem., Int. Ed.* **2004**, *43*, 4656.
14. Suma, K.; Sumiyoshi, Y.; Endo, Y. *J. Am. Chem. Soc*. **2005**, *127*, 14998.
15. Plesničar, B.; Kaiser, S.; Ažman, A. *J. Am. Chem. Soc*. **1973**, *95*, 5476.
16. Cremer, D. *J. Chem. Phys.* **1978**, *69*, 4456.
17. Jackels, C. F.; Phillips, D. H. *J. Chem. Phys.* **1986**, *84*, 5013.
18. Gonzalez, C.; Theisen, J.; Zhu, L.; Schlegel, H. B.; Hase, W. L.; Kaiser, E. W. *J. Phys. Chem.* **1991**, *95*, 6784.
19. Jackels, C. F. *J. Chem. Phys.* **1993**, *99*, 5768.
20. Koller, J.; Plesnièar, B. *J. Am. Chem. Soc*. **1996**, *118*, 2470.
21. Wu, A.; Cremer, D.; Gauss, J. *J. Phys. Chem. A* **2003**, *107*, 8737.
22. Cerkovnik, J.; Tuttle, T.; Kraka, E.; Lendero, N.; Plesničar, B.; Cremer, D. *J. Am. Chem. Soc.* **2006**, *128*, 4090.
23. Kovačic, S.; Koller, J.; Cerkovnik, J.; Tuttle, T.; Plesničar, B. *J. Phys. Chem. A* **2008**, *112*, 8129.
24. Denis, P. A.; Ornella, F. R. *J. Phys. Chem. A* **2009**, *113*, 499.
25. Tuttle, T.; Cerkovnik, J.; Koller, J.; Plesničar, B. *J. Phys. Chem. A* **2010**, *114*, 8003.
26. (a) Becke, A. D. *J. Chem. Phys*. **1993**, *98*, 5648. (b) Lee, C.; Yang, W.; Parr, R. G. *Phys. Rev.* **1988**, *B37*, 785.
27. (a) Dunning, T. H. *J. Chem. Phys.* **1989**, *90*, 1007. (b) Kendall, R. A.; Dunning, T. H.; Harrison, R. J. *J. Chem. Phys*. **1992**, *96*, 6796.
28. Yanai, T.; Tew, D. P.; Handy, N. C. *Chem. Phys. Lett.* **2004**, *393*, 51.
29. Vydrov, O. A.; Scuseria, G. E. *J. Chem. Phys.* **2006**, *125*, 234109.
30. Chai, J. D.; Head-Gordon, M. *Phys. Chem. Chem. Phys.* **2008**, *10*, 6615.
31. Frisch, M. J.; Trucks, G. W.; Schlegel, H. B.; Scuseria, G. E.; Robb, M. A.; Cheeseman, J. R.; Scalmani, G.; Barone, V.; Mennucci, B.; Petersson, G. A.; Nakatsuji, H.; Caricato, M.; Li, X.; Hratchian, H. P.; Izmaylov, A. F.; Bloino, J.; Zheng, G.; Sonnenberg, J. L.; Hada, M.; Ehara, M.; Toyota, K.; Fukuda, R.; Hasegawa, J.; Ishida, M.; Nakajima, T.; Honda, Y.; Kitao, O.; Nakai, H.; Vreven, T.; Montgomery, J. A.; Peralta, J. E., Jr.; Ogliaro, F.; Bearpark, M.; Heyd, J. J.; Brothers, E.; Kudin, K. N.; Staroverov, V. N.; Kobayashi, R.; Normand, J.; Raghavachari, K.; Rendell, A.; Burant, J. C.; Iyengar, S. S.; Tomasi, J.; Cossi, M.; Rega, N.; Millam, J. M.; Klene, M.; Knox, J. E.; Cross, J. B.; Bakken, V.; Adamo, C.; Jaramillo, J.; Gomperts, R.; Stratmann, R. E.; Yazyev, O.; Austin, A. J.; Cammi, R.; Pomelli, C.; Ochterski, J. W.; Martin, R. L.; Morokuma, K.; Zakrzewski, V. G.; Voth, G. A.; Salvador, P.; Dannenberg, J. J.; Dapprich, S.; Daniels, A. D.; Farkas, Ö.; Foresman, J. B.; Ortiz, J. V.; Cioslowski, J.; Fox, D. J. *Gaussian 09, Revision A*; Gaussian, Inc., Wallingford CT, 2009.
32. Boys, S. F.; Bernardi, F.; Boys, S. F.; Bernardi, F. *Mol. Phys.* **1970**, *19*, 553.
33. Farrugia, L. J. *J. Appl. Cryst.* **1997**, *30*, 565.